

Estimation of a Long-Term Variation of a Magnetic-Storm Index Using the Merging Particle Filter

Shin'ya NAKANO^{†**a)}, *Nonmember and* Tomoyuki HIGUCHI^{†*}, *Member*

SUMMARY The D_{st} index is the most popular measure of a scale of magnetic storms, and it is widely used as a monitor of the conditions of the Earth's magnetosphere. Since the D_{st} index contains contributions from multiple magnetospheric phenomena, it is important to distinguish each of the contributions in order to obtain meaningful information about the conditions of the magnetosphere. There have been several efforts which modeled temporal evolution of the D_{st} index empirically, and these empirical models consider some contributions separately. However, they take only short-term variations into account, and contributions from phenomena which show long-term variations are neglected. In the present study, we have developed a technique for estimating the component of long-term variations of the D_{st} index using solar wind data and a nonlinear empirical model. The newly-developed technique adopts an algorithm which is similar to the particle filter. This algorithm allows an on-line processing of a long sequence of D_{st} data, which would enable a real-time estimation of system variables in a nonlinear system model. The estimates of the long-term variations can be used for accurate estimation of other contributions to the D_{st} index, which would provide credible information about the conditions of the magnetosphere. The framework proposed in the present study could be applied for the purpose of continuous real-time monitoring of the environment of the magnetosphere.

key words: merging particle filter, time-series analysis, geomagnetic data

1. Introduction

Magnetic storm is a global phenomenon which causes great decrease in the magnetic field on the ground at low and mid latitudes. The degree of the decrease is commonly measured by D_{st} index [1], which is derived from magnetic-field data at four different ground observatories at mid latitudes. The D_{st} index represents a deviation of the magnetic field at low latitudes from a normal state. The value of D_{st} is thus near zero in a normal state. During magnetic storm, it decreases typically by 50–100 nT and by hundreds of nT for strong magnetic storm. The D_{st} index is calculated for every hour, and its hourly data have been accumulated and published for about 50 years since 1957.

It is widely accepted that the decrease of D_{st} index during magnetic storm is caused by an electric current flowing westward in the magnetosphere, which is called the ring current (Fig. 1; see also, e.g., [2]). It is also well known that an electric current flowing eastward on the outer boundary of the magnetosphere, which is called the magnetopause

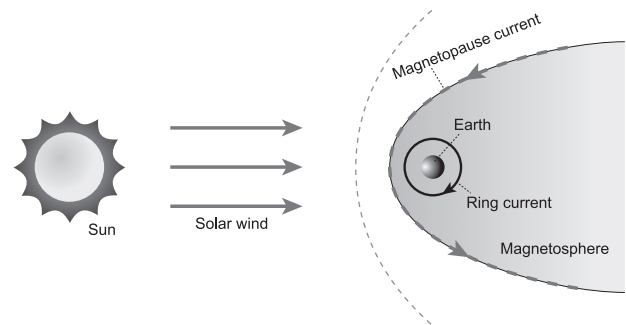


Fig. 1 Schematic picture of the sun-earth system which is focused on in the present paper. This picture is a projection onto the Earth's equatorial plane.

current, also has a significant effect on the value of D_{st} as depicted in Fig. 1. The enhancement of the magnetopause current causes the increases of D_{st} , while the enhancement of the ring current causes the decrease of D_{st} . Hence, the variations of D_{st} are mostly a mixture of the ring current effect (RC effect) and the magnetopause current effect (MPC effect).

The variations of the ring current and the magnetopause current are closely associated with the conditions of the solar wind, which streams outward from the sun, although these two currents depend on different parameters of the solar wind. Burton et al. [3] have empirically modeled the temporal evolution of the D_{st} index using some solar wind parameters. They decomposed the D_{st} variations into the RC effect and the MPC effect, and then consider the temporal variation of each of two effects separately. They assumed the MPC effect to be given as a function of one of the solar-wind parameters, the solar-wind dynamic pressure P_d . The RC effect was described as a nonlinear evolutive system which requires the solar-wind electric field as an input.

Their model (hereafter we will refer to it as the Burton's model) was constructed under the assumption that all the variations of D_{st} are due to the RC effect and/or the MPC effect, and they assumed other contributions to the D_{st} index to be constant, that is, independent from time. However, it is not trivial whether a variation of another contribution is really negligible or not. In particular, a long-term magnetic field variation which can not be represented by the Burton's model might make some significant influence over the D_{st} index. As a matter of fact, we can estimate whether another factor may significantly contribute to D_{st} variations

Manuscript received December 5, 2008.

Manuscript revised March 7, 2009.

[†]The authors are with the Institute of Statistical Mathematics, ROIS, Tokyo, 106–8569 Japan.

^{*}The authors are also with Japan Science and Technology Agency, Kawaguchi-shi, 332–0012 Japan.

a) E-mail: shiny@ism.ac.jp

DOI: 10.1587/transinf.E92.D.1382

on the basis of the Burton’s model itself using long-term data of the D_{st} index and the solar wind.

The purpose of the present paper is to show how we can evaluate another contribution to D_{st} variations and to estimate how large such a contribution is. The estimation of another contribution is conducted using the merging particle filter (MPF) [4]. This algorithm is applicable to nonlinear system models like the Burton’s model and it is effective for applying to a very long-term sequence of data because it is an on-line algorithm which can process long-term data sequentially.

2. Base Model of the Temporal Variation of the D_{st} Index

The D_{st} index is influenced by both the RC effect and the MPC effect. Burton et al. took an approach to model the MPC effect as the first step and then eliminate it from D_{st} to obtain a pure RC effect:

$$D_{RC}(nT) = D_{st} - b\sqrt{P_d} + c \tag{1}$$

where D_{RC} represents the pure RC effect, P_d denotes the dynamic pressure of the solar wind which is observed by spacecraft out of the magnetosphere, and b and c are the parameters which should be given a priori. The second term in the right-hand side of this equation, $b\sqrt{P_d}$, corresponds to the MPC effect, and the third term c corresponds to other contributions than the RC effect and the MPC effect. This means that the Burton’s model assumes that the MPC effect is given by $b\sqrt{P_d}$ and that other contributions is given by the constant c . The temporal evolution of the pure RC effect D_{RC} can then be modeled as follows:

$$\frac{\Delta D_{RC}}{\Delta t} = Q - \frac{D_{RC}}{\tau} \tag{2}$$

where the parameters Q and τ should be given a priori.

The original paper by Burton et al. provided the optimal value of each constant coefficient in Eqs. (1) and (2). However, the optimal values have been revised by O’Brien and McPherron (2000) [5] using a much longer term of the data. According to them, the parameters b and c in Eq. (1) can be given as constants:

$$b = 7.26 \text{ nT/nPa}^{-1/2} \tag{3}$$

$$c = 11 \text{ nT}. \tag{4}$$

The parameter Q , which represents the evolution of D_{RC} , can be given as follows:

$$Q(\text{nT/hour}) = -4.4 H(E - 0.49) \tag{5}$$

where H denotes the Heaviside function as

$$H(x) = \begin{cases} 1 & \text{if } x \geq 0 \\ 0 & \text{otherwise.} \end{cases} \tag{6}$$

The variable E is given as

$$E = vB_s \tag{7}$$

where v is the solar-wind velocity and B_s is the southward component of the solar-wind magnetic field. Both v and B_s can be observed by spacecraft out of the magnetosphere as well as P_d . Finally, τ is given as follows:

$$\tau(\text{hours}) = 2.4 \exp\left(\frac{9.74}{4.69 + H(E)}\right). \tag{8}$$

Once an initial value of the D_{st} index is given, we can predict the evolution of D_{st} sequentially using the model given by Eqs. (1) and (2) as long as the solar-wind data are available. Hence, by comparing the prediction with the actual D_{st} values, we can validate the Burton’s model and the values of coefficients obtained by O’Brien and McPherron and evaluate contributions from other factors than the RC effect and the MPC effect. In the following sections, we perform the prediction by putting the solar-wind data into the Burton’s model.

3. Modeling of the System

3.1 System Model

In order to perform the prediction of the D_{st} index, we construct a state space model on the basis of the Burton’s model. We decompose a state of D_{st} at time t into three components as

$$D_{st}^t = D_{RC}^t + D_{MPC}^t + D_{res}^t \tag{9}$$

where D_{st}^t denotes a model D_{st} value at time t , D_{RC}^t denotes the RC effect on D_{st} , D_{MPC}^t denotes the MPC effect, and D_{res}^t denotes a residual effect other than the RC and MPC effects on D_{st} , which corresponds to $-c$ in Eq. (1) and is of our main interest in the present paper.

According to Eqs. (2) and (5), we describe a transition of a state of D_{RC} for an hour as

$$D_{RC}^t = D_{RC}^{t-1} - 4.4 H(E^{t-1} - 0.49) - \frac{D_{RC}^{t-1}}{\tau}. \tag{10}$$

The MPC effect D_{MPC}^t is assumed to be given as a function of P_d^t as

$$D_{MPC}^t = b\sqrt{P_d^t}. \tag{11}$$

As for a transition of a state of D_{res} , two models are considered in order to evaluate whether a variation of D_{res} is negligible or not. One model assumes D_{res} to be constant as

$$D_{res}^t = -11. \tag{12}$$

according to Eq. (4). The other model is given as

$$D_{res}^t \sim N(D_{res}^{t-1}, 0.01). \tag{13}$$

We also consider state transitions of the two solar-wind

parameters P_d and E . As described above, these two parameters can be observed by spacecraft. However, spacecraft basically observe local structures of the solar wind and the local structures observed by spacecraft do not necessarily agree with large-scale solar-wind structures which controls the conditions of the Earth's magnetosphere. Then, we assume that 'effective' P_d and E are uncertain and we include them in variables to be estimated. Thus, it is necessary to model the state transitions of them. The state of P_d at time t is assumed to obey a log-normal distribution as

$$\log P_d^t \sim N(\log P_d^{t-1}, 0.02) \quad (14)$$

because the solar-wind dynamic pressure P_d can not be less than zero. The variance of P_d was determined by a maximum-likelihood method using a set of OMNI2 hourly solar-wind data \bar{P}_d . The OMNI2 solar-wind data were provided on the OMNIWeb database of National Space Science Data Center, NASA (<http://omniweb.gsfc.nasa.gov/>) and they are also referred to Sect. 3.2. A transition of E is represented using a Cauchy distribution in order to allow large jumps which are sometimes observed in E . We assume that E^t obey the Cauchy distribution with a location parameter of E^{t-1} and a scale parameter of 1. The scale parameter for the transition of E are given subjectively. However, since it is associated with short-term variations, it does not make any significant effects on the estimates of D_{res} . In addition, we assume that τ is time-dependent. We give τ^t as

$$\tau^t = 2.4 \exp\left(\frac{9.74}{4.69 + H(E^{t-1})}\right) \quad (15)$$

where

$$E^{t-1} \sim N(E^{t-1}, 0.25). \quad (16)$$

3.2 Observation Model

From the system described above, we can obtain observations of three variables. Space craft observations provide the data of P_d and E at each hour, although these data are sometimes lost. We define the observation model of P_d and E at each hour as

$$\bar{P}_d^t \sim N(P_d^t, 1) \quad (17)$$

$$\bar{E}^t \sim N(E^t, 4) \quad (18)$$

where \bar{P}_d^t and \bar{E}^t denote the observations of P_d and E at each hour, respectively. In this study, we refer to the OMNI2 solar-wind hourly data as the data of \bar{P}_d^t and \bar{E}^t . Although the original OMNI2 data do not contain \bar{E}^t data, we generate \bar{E}^t data from data of the solar-wind velocity \bar{v}^t and the southward component of the solar-wind magnetic field \bar{B}_z^t as $\bar{E}^t = \bar{v}^t \bar{B}_z^t$. We can also use the values of the D_{st} index at each hour. The data of the D_{st} index are provided by Data Analysis Center for Geomagnetism and Space Magnetism, Kyoto University. The observation model of the D_{st} index is defined as follows:

$$\begin{aligned} \bar{D}_{st}^t &= D_{st}^t + w_{D_{st}}^t \\ &= D_{RC}^t + b \sqrt{P_d^t} + D_{res}^t + w_{D_{st}}^t \end{aligned} \quad (19)$$

where \bar{D}_{st}^t denotes the observed D_{st} index and $w_{D_{st}}^t$ is the observation error contained in the D_{st} data which obeys the normal distribution $N(0, 25)$.

3.3 State Space Model

For the convenience in the following section, we define a state vector as follows:

$$\mathbf{x}_t = \begin{pmatrix} D_{RC}^t \\ D_{res}^t \\ P_d^t \\ E^t \\ \tau^t \end{pmatrix}. \quad (20)$$

Since the MPC effect D_{MPC}^t is assumed to be given as a function of P_d^t , D_{MPC}^t is not included in a state vector. Using this state vector, we can represent a transition of a state \mathbf{x}_t just by a conditional distribution as

$$\mathbf{x}_t \sim p(\mathbf{x}_t | \mathbf{x}_{t-1}). \quad (21)$$

where $p(\mathbf{x}_t | \mathbf{x}_{t-1})$ can be defined by combining Eqs. (10)–(16). We also define an observation vector \mathbf{y}_t as

$$\mathbf{y}_t = \begin{pmatrix} \bar{D}_{st}^t \\ \bar{P}_d^t \\ \bar{E}^t \end{pmatrix}. \quad (22)$$

However, the data of \bar{P}_d^t and \bar{E}^t are sometimes missing as mentioned above. In such cases, we redefine an observation vector \mathbf{y}_t as

$$\mathbf{y}_t = \begin{pmatrix} \bar{D}_{st}^t \end{pmatrix}. \quad (23)$$

In either case, the observation model described in Sect. 3.2 can be written as

$$\mathbf{y}_t \sim p(\mathbf{y}_t | \mathbf{x}_t). \quad (24)$$

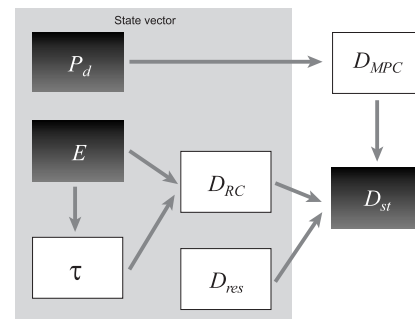


Fig. 2 Dependencies among the variables considered in the present study. The variables which can be observed are indicated by black boxes with white letters.

In ordinary cases, $p(\mathbf{y}_t|\mathbf{x}_t)$ can be defined by combining Eqs. (17)–(19). If the data of either \bar{P}_d^t or \bar{E}^t are missing, only Eq. (19) is evaluated; that is, $p(\mathbf{y}_t|\mathbf{x}_t)$ is determined from Eq. (19).

Figure 2 illustrates the dependencies among the variables considered in the present study. The variables included in the state vector \mathbf{x}_t are enclosed within a shaded box. The observable variables are indicated by black boxes with white letters.

4. Algorithm

We conduct the estimation of the value of the state vector \mathbf{x}_t at each hour from the observations \mathbf{y}_t on the basis of the system and observation models described in the previous section. As the system model described above is nonlinear, the estimation of a state is done using the merging particle filter (MPF) [4], which is applicable even to nonlinear system models. The MPF is an algorithm based on the particle filter (PF) [6]–[8]. The MPF provides an approximation of the posterior probability density function given a sequence of observations $\{\mathbf{y}_1, \dots, \mathbf{y}_T\}$, like the PF. However, it is much more efficient than the normal PF. In the following, the algorithm of the MPF is briefly reviewed.

In the MPF, a probability density function (PDF) $p(\mathbf{x})$ is approximated by a set of N samples $\{\mathbf{x}^{(1)}, \dots, \mathbf{x}^{(N)}\}$ as also done in the particle filter as

$$p(\mathbf{x}) \approx \frac{1}{N} \sum_{i=1}^N \delta(\mathbf{x} - \mathbf{x}^{(i)}). \tag{25}$$

Each sample is called a ‘particle’ and an approximation of a PDF using a set of particles is called a ‘particle approximation’. In the normal PF, a set of particles for representing a posterior PDF contains many duplicates of the same particle, which causes highly redundant computational cost. On the other hand, in the MPF, each particle is generated by merging multiple samples in order to maintain the diversity of particles. This allows us to reduce the redundant computational cost.

We sequentially obtain particle approximations of a predictive PDF $p(\mathbf{x}_t|\mathbf{y}_{1:t-1})$ and a filtered PDF $p(\mathbf{x}_t|\mathbf{y}_{1:t})$ at each time step as follows. Suppose that a PDF $p(\mathbf{x}_{t-1}|\mathbf{y}_{1:t-1})$, which is a posterior PDF given the observations until time $t - 1$, is approximated by a set of particles $\{\mathbf{x}_{t-1|t-1}^{(i)}\}_{i=1}^N$ as

$$p(\mathbf{x}) \approx \frac{1}{N} \sum_{i=1}^N \delta(\mathbf{x}_{t-1} - \mathbf{x}_{t-1|t-1}^{(i)}). \tag{26}$$

If we obtain a set of particle where each particle $\mathbf{x}_{t|t-1}^{(i)}$ is a sample taken from a conditional distribution $p(\mathbf{x}_t|\mathbf{x}_{t-1|t-1}^{(i)})$, this set of samples $\{\mathbf{x}_{t|t-1}^{(i)}\}_{i=1}^N$ offers a particle approximation of a predictive PDF at the next time, $p(\mathbf{x}_t|\mathbf{y}_{1:t-1})$, as

$$p(\mathbf{x}_t|\mathbf{y}_{1:t-1}) \approx \frac{1}{N} \sum_{i=1}^N \delta(\mathbf{x}_t - \mathbf{x}_{t|t-1}^{(i)}). \tag{27}$$

An approximation of the filtered PDF $p(\mathbf{x}_t|\mathbf{y}_{1:t})$ can be obtained by incorporating an observation \mathbf{y}_t into the particle approximation of a predictive PDF $\{\mathbf{x}_{t|t-1}^{(i)}\}_{i=1}^N$ as follows:

$$\begin{aligned} p(\mathbf{x}_t|\mathbf{y}_{1:t}) &= \frac{p(\mathbf{x}_t|\mathbf{y}_{1:t-1}) p(\mathbf{y}_t|\mathbf{x}_t)}{\int p(\mathbf{x}_t|\mathbf{y}_{1:t-1}) p(\mathbf{y}_t|\mathbf{x}_t) d\mathbf{x}_t} \\ &\approx \frac{1}{\sum_j p(\mathbf{y}_t|\mathbf{x}_{t|t-1}^{(j)})} \sum_{i=1}^N p(\mathbf{y}_t|\mathbf{x}_{t|t-1}^{(i)}) \delta(\mathbf{x}_t - \mathbf{x}_{t|t-1}^{(i)}) \\ &= \sum_{i=1}^N w_i \delta(\mathbf{x}_t - \mathbf{x}_{t|t-1}^{(i)}) \end{aligned} \tag{28}$$

where $p(\mathbf{y}_t|\mathbf{x}_{t|t-1}^{(i)})$ is the likelihood of $\mathbf{x}_{t|t-1}^{(i)}$ given the data \mathbf{y}_t , which can be calculated according to Eq. (24). The weight w_i is defined as

$$w_i = \frac{p(\mathbf{y}_t|\mathbf{x}_{t|t-1}^{(i)})}{\sum_j p(\mathbf{y}_t|\mathbf{x}_{t|t-1}^{(j)})}. \tag{29}$$

Although Eq. (28) offers an approximation of the filtered PDF $p(\mathbf{x}_t|\mathbf{y}_{1:t})$, we generate a new set of particles $\{\mathbf{x}_{t|t}^{(i)}\}_{i=1}^N$ which represents the filtered PDF in the following form:

$$p(\mathbf{x}_t|\mathbf{y}_{1:t}) \approx \frac{1}{N} \sum_{i=1}^N \delta(\mathbf{x}_t - \mathbf{x}_{t|t}^{(i)}). \tag{30}$$

In the MPF, each particle for representing the filtered PDF is obtained by combining multiple particles taken from a set of particles for representing the predictive PDF; that is, a particle $\mathbf{x}_{t|t}^{(i)}$ is obtained from multiple samples from $\{\mathbf{x}_{t|t-1}^{(i)}\}_{i=1}^N$. Here the number of particles to be combined is taken as 3. Then, in order to obtain a set of N particles $\{\mathbf{x}_{t|t}^{(i)}\}_{i=1}^N$, it is necessary to draw $3N$ samples with weights of $w_i \{\hat{\mathbf{x}}_{t|t}^{(1,1)}, \dots, \hat{\mathbf{x}}_{t|t}^{(3,1)}, \dots, \hat{\mathbf{x}}_{t|t}^{(1,N)}, \dots, \hat{\mathbf{x}}_{t|t}^{(3,N)}\}$. Each particle in the new set, $\{\mathbf{x}_{t|t}^{(i)}\}$, is generated as a weighted sum of 3 samples contained in this $3N$ samples as:

$$\mathbf{x}_{t|t}^{(i)} = \sum_{j=1}^n \alpha_j \hat{\mathbf{x}}_{t|t}^{(j,i)}. \tag{31}$$

The set of weights $\{\alpha_j\}_{j=1}^n$ in Eq. (31) is set to satisfy

$$\sum_{j=1}^n \alpha_j = 1 \tag{32a}$$

$$\sum_{j=1}^n \alpha_j^2 = 1 \tag{32b}$$

where $\alpha_j \in \mathcal{R}$ for all j . Eqs. (32a) and (32b) ensures that the new set of particles $\{\mathbf{x}_{t|t}^{(i)}\}_{i=1}^N$ has asymptotically the same average and covariance of the filtered PDF $p(\mathbf{x}_t|\mathbf{y}_{1:t})$ for $N \rightarrow \infty$.

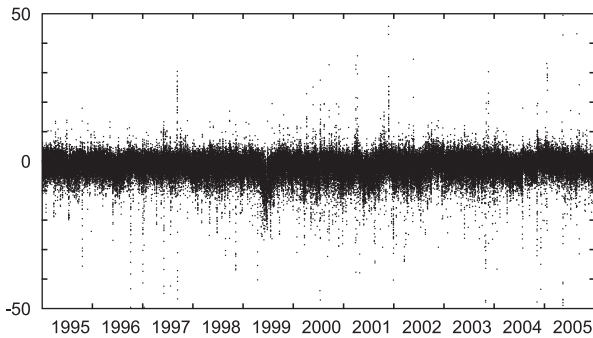


Fig. 3 Difference between the model D_{st} and the actual D_{st} for the case that D_{res} is assumed to be constant.

5. Result

We estimated the temporal evolution of the state vector \mathbf{x}_t for the period from 1995 to 2005. The estimation was performed for the period from 1995 because many of the OMNI2 solar-wind data are missed before 1995. An estimate of \mathbf{x}_t at each time step was provided from the ensemble mean of particles $\{\mathbf{x}_{t|t}^{(i)}\}_{i=1}^N$, which approximates a filtered PDF $p(\mathbf{x}_t | \mathbf{y}_{1:t})$. The number of particles N used for the estimation was 1600. In order to evaluate whether the temporal evolution was successfully estimated or not, we compare the D_{st} evolution estimated using the MPF with a sequence of the real D_{st} data.

Figure 3 shows difference between the real D_{st} data and the model D_{st} for the case that D_{res} is assumed to be constant where positive means that the model D_{st} is larger than the actual D_{st} . Although the difference sometimes becomes larger than 20 nT, it mostly varies with the amplitude of about 10 nT during the period from 1995 to 2005. However, some long-term variation is also seen in this figure. In particular, the model D_{st} is prominently smaller than the actual D_{st} around the middle of 1999. Figure 4 compares the model D_{st} for constant D_{res} with the actual D_{st} during one year from January 1999 to December 1999. The gray line indicates the actual D_{st} and the black line indicates the model D_{st} . From the end of May to July, the model D_{st} underestimated the actual D_{st} by about 10 nT.

Figure 5 compares the model D_{st} for the case that D_{res} is variable according to Eq. (13) with the actual D_{st} for the period from January 1999 to December 1999. The gray line indicates the actual D_{st} and the black line indicates the model D_{st} as in Fig. 4. The model D_{st} well agree with the actual D_{st} . Indeed, while the log-likelihood of the model based on Eq. (12) was about -1.8×10^{-8} , the log-likelihood of the model based on Eq. (13) was about -1.5×10^{-5} . The dashed line shows the estimated D_{res} . The residual effect D_{res} exceeds zero from the middle of the May to the middle of the September, while the empirical model assumes that D_{res} is negative ($D_{res} = -11$ nT). This result means that the residual effect is more variable than assumed by the previous studies. The Burton's model sometimes overestimate D_{res} and sometimes underestimate D_{res} by tens of nT, which

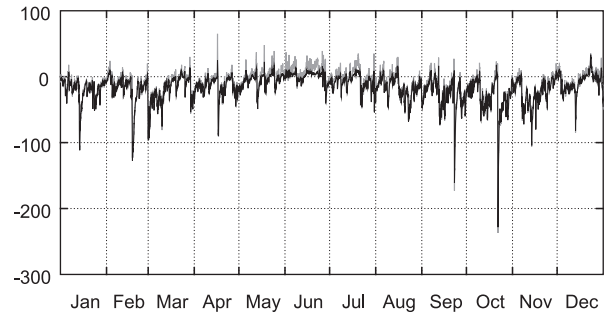


Fig. 4 Comparison between the model D_{st} (black solid line) and the actual D_{st} (gray solid line) from January 1999 to December 1999 for the case that D_{res} is assumed to be constant.

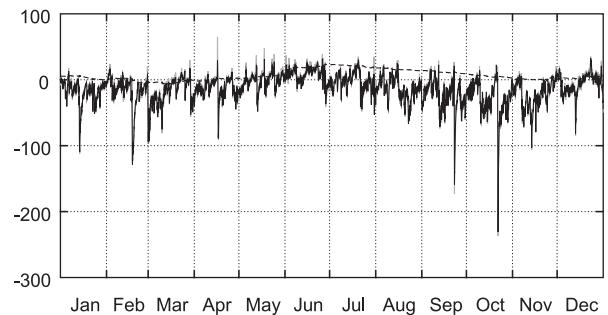


Fig. 5 Comparison between the model D_{st} (black solid line) and the actual D_{st} (gray solid line) from January 1999 to December 1999 for the case that D_{res} is modeled according to Eq. (13). The estimated D_{res} (see text) is also shown in a dashed line.

inevitably causes misestimation of D_{RC} . As described in Introduction, D_{st} varies typically by 50–100 nT during magnetic storms. Thus, the improvement of the estimation of D_{res} is not negligible in order to evaluate the RC effect using the D_{st} index.

6. Concluding Remarks

We have presented a new technique to estimate the contribution from an unconsidered factor in the Burton's model which describes temporal evolution of a measure of magnetic storms, the D_{st} index. The estimation is performed using the merging particle filter which is applicable to nonlinear system models like the Burton's model. By considering a long-term variation in addition to the RC effect and the MPC effect which are already considered in the Burton's model, the agreement between the model D_{st} value and the actually observed D_{st} value is greatly improved. This fact means that a long-term residual effect D_{res} significantly contributes to the D_{st} index. In order to accurately estimate the temporal variation of the RC effect D_{RC} , we need to accurately estimate the variation of D_{res} . Thus, the technique which we presented above would serve as an important tool for analyzing the temporal evolution of D_{RC} index.

Recently, continuous monitoring of magnetic storm activity becomes important because it is associated with the environment of the magnetosphere where many spacecraft

operate and with the conditions of the ionosphere. Thus, a real-time monitor of magnetic storm activity and the ring current is important. In the present study, we adopted the merging particle filter (MPF). The MPF is an on-line algorithm applicable for processing even real-time data and it enables an on-line estimation of the long-term residual effect D_{res} . This on-line estimation provides valuable information for real-time estimation of the ring current variation D_{RC} . Thus, the framework adopted in the present paper could be useful for a real-time monitoring of the magnetospheric environment using the real-time edition of the D_{st} index.

Acknowledgment

This study was partially supported by the Japan Science and Technology Agency (JST) under the Core Research for Evolutional Science and Technology (CREST) program. We are grateful to World Data Center for Geomagnetism, Kyoto University for providing the D_{st} index. We also thank National Space Science Data Center, NASA for providing the OMNI2 solar-wind data.

References

- [1] M. Sugiura and T. Kamei, Equatorial D_{st} index 1957–1986, ISGI Publisher Off., Saint-Maur-des-Fosses, France, 1960.
- [2] W. Baumjohann and R.A. Treumann, Basic space plasma physics, Imperial College Press, London, UK, 1987.
- [3] R.K. Burton, R.L. McPherron, and C.T. Russell, “An empirical relationship between interplanetary conditions and D_{st} ,” J. Geophys. Res., vol.80, pp.4204–4214, 1975.
- [4] S. Nakano, G. Ueno, and T. Higuchi, “Merging particle filter for sequential data assimilation,” Nonlin. Process. Geophys., vol.14, pp.395–408, 2007.
- [5] T.P. O’Brien and R.L. McPherron, “An empirical phase space analysis of ring current dynamics: Solar wind control of injection and decay,” J. Geophys. Res., vol.105, pp.7707–7719, 2000.
- [6] N.J. Gordon, D.J. Salmond, and A.F.M. Smith, “Novel approach to nonlinear/non-Gaussian Bayesian state estimation,” IEE Proc. F, vol.140, pp.107–113, 1993.
- [7] G. Kitagawa, “Monte Carlo filtering and smoothing method for non-Gaussian nonlinear state space model,” Inst. Statist. Math. Res. Memo., no.462, 1993.
- [8] G. Kitagawa, “Monte Carlo filter and smoother for non-Gaussian nonlinear state space models,” J. Comp. Graph. Statist., vol.5, pp.1–25, 1996.



Shin'ya Nakano received the Ph.D. degree in science with a specialty in space physics and geophysics from Kyoto University in 2004. Currently, he is a researcher at the Institute of Statistical Mathematics, Research Organization of Information and Systems, funded by Japan Science and Technology Agency. He is a member of the Society of Geomagnetism and Earth, Planetary and Space Sciences, the Japan Geoscience Union, the American Geophysical Union.



Tomoyuki Higuchi completed his doctoral course in the Department of Geophysics, in 1989 at the University of Tokyo. He holds a Ph.D. degree in Science. Currently, he is a professor in the Department of Statistical Modeling and Vice Director General at the Institute of Statistical Mathematics, Research Organization of Information and Systems. His specialty is statistical analysis, in particular, Bayesian modeling for knowledge discovery. He is a member of the Japan Statistical Society, the Society of Geomagnetism and Earth, Planetary and Space Sciences, the American Geophysical Union, and the American Statistical Association.